

This is a repository copy of *Morphological divergence in giant fossil dormice*.

White Rose Research Online URL for this paper:

<https://eprints.whiterose.ac.uk/166750/>

Version: Accepted Version

---

**Article:**

Hennekam, Jesse, Benson, Roger, Herridge, Victoria et al. (4 more authors) (2020) Morphological divergence in giant fossil dormice. *Proceedings of the Royal Society B: Biological Sciences*. pp. 1-9. ISSN 1471-2954

<https://doi.org/10.1098/rspb.2020.2085>

---

**Reuse**

Items deposited in White Rose Research Online are protected by copyright, with all rights reserved unless indicated otherwise. They may be downloaded and/or printed for private study, or other acts as permitted by national copyright laws. The publisher or other rights holders may allow further reproduction and re-use of the full text version. This is indicated by the licence information on the White Rose Research Online record for the item.

**Takedown**

If you consider content in White Rose Research Online to be in breach of UK law, please notify us by emailing [eprints@whiterose.ac.uk](mailto:eprints@whiterose.ac.uk) including the URL of the record and the reason for the withdrawal request.

**Title: Morphological divergence in giant fossil dormice**

Authors: Jesse J. Hennekam<sup>1</sup>, Roger B.J. Benson<sup>2</sup>, Victoria L. Herridge<sup>3</sup>, Nathan Jeffery<sup>4</sup>, Enric Torres-Roig<sup>5</sup>, Josep Antoni Alcover<sup>6</sup>, Philip G. Cox<sup>1,7</sup>

Affiliations:

<sup>1</sup>*Hull York Medical School, University of York, UK*

<sup>2</sup>*Department of Earth Sciences, University of Oxford, UK*

<sup>3</sup>*Natural History Museum, London, UK*

<sup>4</sup>*Department of Musculoskeletal & Ageing Science, Institute of Life Course & Medical Sciences, University of Liverpool, UK*

<sup>5</sup>*Departament de Dinàmica de la Terra i de l'Oceà, Facultat de Ciències de la Terra, Universitat de Barcelona, Barcelona, Spain*

<sup>6</sup>*Departament de Biodiversitat i Conservació, Institut Mediterrani d'Estudis Avançats (CSIC-UIB), Esporles, Mallorca, Spain*

<sup>7</sup>*Department of Archaeology, University of York, UK*

Corresponding author: Jesse J. Hennekam

Address: PalaeoHub, University of York, Wentworth Way, York, YO10 5DD, UK

Email: [jjh556@york.ac.uk](mailto:jjh556@york.ac.uk)

## 1 **Abstract**

2 Insular gigantism – evolutionary increases in body size from small-bodied mainland ancestors - is a  
3 conceptually significant, but poorly studied, evolutionary phenomenon. Gigantism is widespread on  
4 Mediterranean islands, particularly among fossil and extant dormice. These include an extant giant  
5 population of *Eliomys quercinus* on Formentera, the giant Balearic genus †*Hypnomys* and the  
6 exceptionally large †*Leithia melitensis* of Pleistocene Sicily. We quantified patterns of cranial and  
7 mandibular shape and their relationships to head size (allometry) among mainland and insular  
8 dormouse populations, asking to what extent the morphology of island giants is explained by  
9 allometry. We find that gigantism in dormice is not simply an extrapolation of the allometric trajectory  
10 of their mainland relatives. Instead, a large portion of their distinctive cranial and mandibular  
11 morphology resulted from population- or species-specific evolutionary shape changes. Our findings  
12 suggest that body size increases in insular giant dormice were accompanied by evolutionary divergence  
13 of feeding adaptations. This complements other evidence of ecological divergence in these taxa, which  
14 span predominantly faunivorous to herbivorous diets. Our findings suggest that insular gigantism  
15 involves context-dependent phenotypic modifications, underscoring the highly distinctive nature of  
16 island faunas.

17

## 18 **Keywords**

19 Insular Gigantism; Geometric morphometrics; Allometry; Island rule; *Leithia*; *Hypnomys*

20

## 21 **Introduction**

22 Insular gigantism is a widespread macroevolutionary pattern [1,2]. It occurred on many Mediterranean  
23 islands throughout the Neogene and Quaternary, and is known among small mammals including  
24 dormice, hamsters, murids, lagomorphs, shrews and moonrats [3-10]. Despite its prevalence, the  
25 ecological drivers of insular gigantism are rather complex, with climate, island area, availability of

26 resources, and the presence of competitors and predators all proposed to play a part [2, 11-18].  
27 Similarly, the morphological consequences of gigantism are not well understood, and it is not clear  
28 whether giant island species have attained large size via similar evolutionary pathways. This raises the  
29 possibility that insular gigantism does not represent a single well-defined process, but in fact reflects  
30 the outcomes of evolution in a broad set of distinct ecological contexts.

31           Shape changes associated with increasing body size (allometry) are suggested to either result  
32 from optimised functionality based on natural selection, or from constraints that impose fixed or  
33 slowly-evolving allometric trajectories [19]. Allometric constraints will result in shared allometric  
34 patterns ('common allometry') among related species, and provide an expectation that evolution will  
35 proceed along lines of least evolutionary resistance (or "genetic lines of least evolutionary resistance")  
36 [20], represented by a multivariate factor of the genetic or phenotypic variation [21] (but see [22]).  
37 Deviation from these lines might be expected during adaptation to distinct ecological niches, resulting  
38 in functional modification in shape and size. However, the evolvability of allometric relationships, and  
39 therefore the ability of ecological adaptation to cause divergent patterns of phenotypic evolution, is  
40 variable [23,24]: divergence from allometric trajectories may be common on long macroevolutionary  
41 timescales but are rare on shorter timescales.

42           The Island Rule describes extensive variation in both shape and size [1], and suggests a graded  
43 trend from gigantism in small mammals to dwarfism in larger species [13]. The evolutionary timescales  
44 of adaptation to insularity are generally short [25], meaning that divergence from an ancestral  
45 allometric trajectory may be difficult to realise [24]. Nevertheless, the exceptional increase in body size  
46 associated with insular gigantism can result in unexpected morphologies, and evolutionary shifts to  
47 novel ecologies in context of the island setting might also be a powerful driver of evolutionary changes  
48 in morphology via functional adaptation.

49           Dormice (Gliridae) are potent exemplars of the evolutionary 'island effect' of body size  
50 increase, having evolved extraordinary large sizes more frequently than other mammals –and on at  
51 least eight different islands since the beginning of the Miocene [26,27]. Furthermore, giant dormice

52 are known from both the fossil record (e.g. *Hypnomys* spp. from the Balearic Islands and *Leithia* spp.  
53 from Sicily and Malta) and an extant population of *Eliomys quercinus* on the island of Formentera [28].  
54 Dormice therefore provide an ideal study system for addressing key questions regarding insular  
55 gigantism.

56 The fossil giants *Hypnomys* and *Leithia* most likely evolved from a mainland ancestor related  
57 to the genus *Eliomys* (Leithiinae) [29,30,31]. Previous studies uncovered craniomandibular differences  
58 between extant *Eliomys* populations and fossil island genera [31-34]. The possibility that they were  
59 more than simply enlarged forms of their mainland relatives is further supported by the change in  
60 ecological niche displayed by the extant giant population on Formentera, which shows increased  
61 faunivory in its diet [28]. Furthermore, the morphological features of the extinct island giants imply  
62 alternative lifestyles such as increased terrestriality in *Hypnomys* [31] and herbivory in *Leithia* [32].

63 Here, the cranial and mandibular morphology in the extant giant *Eliomys quercinus* from  
64 Formentera and the extinct giant genera *Leithia* and *Hypnomys* are investigated in the context of a  
65 large dataset of non-giant dormouse skulls. *Eliomys quercinus* has a large geographic distribution  
66 across Europe, including several populations on Mediterranean islands. Alongside fossil giants and the  
67 extant giant population on Formentera, non-giant *E. quercinus* still display significant intraspecific size  
68 variations. We aim to understand the transformation of cranial and mandibular form (size and shape)  
69 in giant dormice by investigating the allometric trajectory of non-giant dormice. Characterisation of  
70 the common allometric trajectory within *E. quercinus* populations enables us to distinguish between  
71 morphological differences occurring due to size variations and those potentially related to other  
72 factors. We ask to what extent the cranial and mandibular morphologies of island giant dormice are  
73 predicted by extrapolation of the allometric trajectory for extant non-giant dormice, or whether  
74 additional morphological variation occurs during evolution of giant size – possibly driven by island-  
75 specific shifts in ecology.

76

77 **Material and Methods**

78 *Sample*

79 We analysed the skulls and mandibles of 63 adult specimens (fully erupted third molar) of the extant  
80 species *Eliomys quercinus*. Specimens were from the collections of the Senckenberg Museum,  
81 Frankfurt (SMF), the Muséum National d'Histoire Naturelle, Paris (MNHN) and the Natural History  
82 Museum, London (NHMUK). Table S1 includes a full list of all extant specimens used in this study and  
83 details of our  $\mu$ CT scanning methods are given in Appendix S1. Because only adult individuals were  
84 analysed, our analyses (see below) describe patterns of static allometry.

85 Size variation in *Eliomys* was characterised among geographically separated extant  
86 populations and in fossil giants. We used centroid size (the square root of the summed squared  
87 distances between landmarks and the centroid [35]) derived from our landmark configurations as a  
88 size proxy. Our subsequent analyses focused on quantifying allometry within a single species, *Eliomys*  
89 *quercinus*, the closest living relative of insular giant dormice lineages [29,30,31]. Ideally, we would  
90 compare extinct giant dormice with their specific mainland ancestor populations. However,  
91 phylogenetic relationships among populations of *E. quercinus* are not currently known, let alone the  
92 relationships of mainland populations with extinct island giants.

93 Fossil specimens of the insular species *Hypnomys onicensis*, *H. morpheus* and *Leithia melitensis*  
94 were included in the analyses based on  $\mu$ CT models (Appendix S1), with small missing portions  
95 reconstructed from photogrammetric models of other specimens. The fossil specimens include: a  
96 composite reconstruction of the skull of *L. melitensis* based on specimens present at the Museo  
97 Geologico Gemmellaro (mgupPS 78: 1-5)[32]; the reconstruction of an *L. melitensis* mandible located  
98 at the Museo Universitario di Scienze Della Terra, Rome (MUST R2s26); a well preserved skull of *H.*  
99 *morpheus* from Cova des Coral-loides (unnumbered specimen, under the responsibility of the Heritage  
100 Authorities of the Consell Insular de Mallorca, Palma); and a mostly complete skull of the giant Balearic  
101 dormouse *H. onicensis* in the collection of the Institut Mediterrani d'Estudis Avançats, Esporles,  
102 Mallorca (IMEDEA 106855). Although this specimen is likely a sub-adult, based on size, dental wear  
103 and the unfused skull sutures, it is the most complete skull available of this species.

104

105 *Shape analyses of extant dormice*

106 Anatomical landmarks were recorded from each cranium (42 landmarks) and mandible (19 landmarks)  
107 using Avizo Lite v9.2.0 (Thermo Fisher Scientific, Waltham, MA, USA). The *Arothron* package [36] was  
108 used to import the landmarks into R v3.5.3 [37]. We used 3D geometric morphometrics to characterize  
109 shape variation among extant populations of *E. quercinus* and extinct giants. Generalized Procrustes  
110 Analysis (GPA) was performed, translating the landmark coordinates to the origin, scaling to unit  
111 centroid size, and rotating them to a shared orientation, using a least squares criterion [38,39]. This  
112 analysis separates variation in size (centroid sizes) from variation in shape (Procrustes coordinates) so  
113 they can be treated as individual variables. A Principal Component Analysis (PCA) was performed using  
114 the geometric morphometric R package *Morpho* v2.6 [40], in order to evaluate the data in a lower  
115 dimensional space and identify the largest variances in shape within the dataset.

116

117 *Allometry*

118 Analysis of variance (ANOVA) was used to test the effect of size on adult shape variation (i.e. static  
119 allometry) in *E. quercinus* and the fossil giants. Using the `procD.lm()` function with 999 iterations in the  
120 R package *geomorph* v3.2.0 [41], the following linear model formula was evaluated:  
121  $shape \sim \log_{10}(size)$ , in which size is represented by centroid size. This analysis asks what changes in  
122 cranial or mandibular shape are associated with changes in cranial or mandibular size. Our initial  
123 analyses included a categorical variable differentiating between non-giant and giant dormice for both  
124 the extant dataset (including the extant Formentera giants), as well as the complete dataset (including  
125 the fossil giants). When used as a covariate,  $shape \sim \log_{10}(size) + giant$ , this variable asks whether  
126 giant dormice show specific differences in skull shape compared to non-giant dormice; when used as  
127 an interaction term,  $shape \sim \log_{10}(size) * giant$ , it asks whether the relationship between shape  
128 and size (i.e. its slope) differs between giant and non-giant dormice.

129           Subsequent analyses aimed to quantify the allometric signal among non-giant populations and  
130 therefore used a more restricted sample, excluding giants. The independent effects of population  
131 (defined by geographic location) and sex on shape were evaluated for non-giant *Eliomys* specimens  
132 using the model:  $shape \sim \log_{10}(size) + population + sex$  (Tables S2 and S3). We also asked  
133 whether the effect of allometry varies among populations (Table S1) using the model formula:  
134  $shape \sim \log_{10}(size) * population$ . The significance of coefficients and interaction terms in these  
135 models was assessed using ANOVA with permutation procedures.

136

### 137 *Predicted Shape Model*

138 The allometric relationship defined above can be used to evaluate the extent to which the morphology  
139 of (giant) specimens is explained by their size. A multivariate regression for allometry  $shape \sim size$   
140 can be expressed as  $Y = C + BX + E$  [42], in which  $Y$  is the shape vector,  $C$  is the intercept,  $B$  is  
141 the vector of the regression coefficients for size and represents the angle of the slope of the  
142 multivariate regression line,  $X$  represents centroid size, and  $E$  explains the error term. When using  
143 Procrustes coordinates, the size component  $X$  can be evaluated as the difference between the centroid  
144 size of each specimen and mean centroid size across all specimens. This procedure renders the  
145 intercept term  $C$  redundant with the mean shape from Procrustes superimposition.

146           Our analyses of allometry among non-giant dormice demonstrated a small, but significant,  
147 contribution of population (i.e. geographic location) to cranial and mandibular shape variation (Tables  
148 S2 and S3). Therefore, we used the allometric relationships derived from the model  
149  $shape \sim \log_{10}(size) + population$  among non-giant dormice for the allometric base model in the  
150 subsequent analyses.

151

### 152 *Predicting shape from size.*

153 The base allometric model provides a predicted shape for each specimen based on its size. The  
154 Procrustes coordinates of individual specimens can be projected on to an axis described by the vector



155 of size coefficients,  $B$ , from the multivariate regression [43]. This vector defines an axis in multivariate  
156 space and is equivalent to the common allometric component (CAC) [44]. The orthogonal projection  
157 of specimens onto this axis gives a regression (or CAC) score. The plot of regression score against size  
158 provides a 2D representation of the allometric model. Shape residuals describe how the true shape of  
159 each specimen differs from its predicted shape and are represented in the plot as the vertical (i.e.  
160 shape) deviation of each specimen from the regression line.

161

162 *Predicting size from shape.*

163 The base allometric model can also be used to infer a 'predicted size' for each specimen based  
164 on its shape (Procrustes coordinates). Predicted sizes identify whether the shape of a specific specimen  
165 resembles that of a smaller or a larger specimen. They also allow us to infer a best-fit shape based on  
166 predicted size, representing the shape a specimen would have if it only deviated from allometric  
167 expectations by modification of the position on the allometry line (under the assumption that all shape  
168 variation between specimens is associated with allometry).

169 Predicted sizes were inferred using a custom-written R function: `predict.size()` (Appendix S2).  
170 This function uses the regression vector from the base allometric model to generate a series of  
171 predicted shapes representing individuals of different sizes. These predicted shapes are calculated  
172 using a  $2 \times n$  matrix in which the first row comprises the vector of intercept values and the second row  
173 comprises the coefficients of size in the base allometric model. This was multiplied by an  $m \times 2$  matrix,  
174 in which the first column consists solely of ones and the second column contains an ascending  
175 sequence of size values of length  $m$ . Our `predict.size()` function by default sets the upper size limit to  
176 1.5 times the size of the largest individual within the dataset. The resulting matrix is transformed to an  
177 array based on the number of landmarks within the configuration and its dimensionality, creating a  
178 dataset comprising a sequence of shape coordinate data associated with the allometric trajectory per  
179 increment of size. This approach can be used to generate predicted sizes of external specimens that

180 were not included in the base allometric model, provided they are superimposed on the consensus  
181 shape of this model.

182         The extent to which specimen shapes differ from the shapes predicted by allometry, given  
183 their predicted sizes, provides a measure of the amount of shape difference between specimen shapes  
184 and their deviation from allometric expectations (given actual sizes) that cannot be explained simply  
185 by modification of position on the allometry line. It therefore allows us to quantify the amount of non-  
186 allometric shape deviation exhibited by a specimen, which might, for example, reflect individual-,  
187 population- or species-specific variation. This is calculated as the orthogonal projection of specimen  
188 shapes on the regression vector. Our `predict.size()` function estimates this by evaluating the Procrustes  
189 distances between the actual specimen shape and every proposed shape on the regression vector. The  
190 proposed shape with the shortest Procrustes distances is the indicator for predicted size.

191         The relationship between predicted and actual size for each specimen was displayed  
192 graphically via a 'predicted size versus actual size', or PSvAS, plot. This method is complementary to  
193 existing allometric methods, and allows for the evaluation of the shape of individual specimens with  
194 respect to the base allometric model. A line with intercept = 0 and slope = 1 on this plot represents  
195 shapes with predicted sizes that match their actual sizes. This identity line divides the graph into two  
196 sections, the lower-right indicating specimens with a centroid size exceeding the predicted centroid  
197 size based on shape, and the upper-left including specimens with larger predicted sizes than the actual  
198 centroid size.

199

#### 200 *Application of PSvAS to the dormouse dataset*

201 The PSvAS method was used for analysing the shape of giant dormice, based on an allometric base  
202 model including non-giant, extant *Eliomys quercinus* specimens. The fit of the fossil and extant giants  
203 within the model was analysed to determine whether certain morphological features are in line with  
204 the allometric predictions, or can be considered distinct characteristics for giants. Because the giant  
205 dormice are considerably different in size and shape compared to non-giant *Eliomys*, including such

206 specimens will affect the GPA and therefore influence the inferred allometric component. Instead,  
207 these specimens were superimposed to the consensus shape of the base model rather than being  
208 included in the original GPA.

209

## 210 **Results**

### 211 *Shape variation in dormice.*

212 Principal component ordinations for both the cranial and mandibular dataset depict a clear signal  
213 related to the distinctive morphology of giant species (Figure 1A,D). The first principal component is  
214 correlated with size variation of extant, non-giant populations, with more positive values being  
215 associated with larger individuals. The second principal component appears to distinguish between  
216 extant (negative values) and fossil (positive values) giants. Overall, these patterns are more defined in  
217 the cranial analyses.

218

### 219 *Size-shape relationships*

220 Our initial analyses of allometry demonstrate statistical significance for an independent variable  
221 distinguishing between giant and non-giant dormice both when including only extant populations, and  
222 for the complete dataset including fossil specimens (Tables S4 and S5). This indicates a role for non-  
223 allometric shape variation during the origin of giant dormouse cranial and mandibular morphology.  
224 The interaction term of this variable is non-significant for the extant dataset, but significant for the  
225 complete dataset including fossil specimens. This indicates that the relationship between shape and  
226 size among living and extinct giants from multiple islands is different to that among non-giant  
227 populations (Figure 1B,E). Our subsequent analyses further interrogate and characterize these  
228 differences.

229

### 230 *Allometric base model*

231 ANOVAs demonstrate statistically significant effects of size and population on the allometric  
232 base models for both mandibular and cranial shape (Tables S2 and S3). The effect of sex (21 females;  
233 24 males; 1 unknown) on mandibular and cranial shape is non-significant and sex was therefore was  
234 excluded from further analyses ( $p = 0.188$ ;  $p = 0.271$ ). The interaction term between size and  
235 population is also non-significant (mandible:  $p = 0.548$ ; skull:  $p = 0.346$ ), indicating that there is no  
236 evidence for population-specific allometric effects in non-giant dormice. Thus, the best model is:  
237  $shape \sim \log_{10}(size) + population$ ; which explains 53% of the total variation in both the  
238 mandibular and cranial datasets (Tables S2 and S3). The PSvAS model was used to evaluate the shape  
239 of giant dormice crania and mandibles with respect to this allometric model, based solely on non-giant  
240 dormice (Figure 1C,F).

241

#### 242 *Predicted Size versus Actual Size*

243 The PSvAS plots describe the relationship between the size of each specimen and its predicted  
244 size based on shape in context of the allometric model (Figures 1C,F and 2). Giant specimens in these  
245 graphs are located firmly below the identity line, indicating that their shapes resemble the crania and  
246 mandibles of smaller individuals (Table S6). This effect is generally more pronounced for mandibles  
247 than for crania (Figure 1). Furthermore, the larger fossil specimens deviate more from the identity line  
248 compared to the extant giants from Formentera.

249

#### 250 *Predicted and actual morphology of giant dormice*

251 Procrustes distances quantify the difference between the actual shape of giants and the  
252 predicted shapes based on the allometric model (Table S6). Differences between giant shapes and  
253 expectations under the allometric base model are relatively large (cranium: 0.07 – 0.18, mandible: 0.08  
254 – 0.22), especially within the fossil genera *Hypnomys* and *Leithia*. These differences remain large even  
255 when using the predicted (best fit) size given shape (Table S6; cranium: 0.07 – 0.13, mandible: 0.06 –  
256 0.12), indicating that the actual morphology of giants is rather poorly predicted by the allometric

257 model, suggesting that giant dormouse cranial and mandibular morphologies originated via largely  
258 non-allometric evolutionary processes.

259         Based on both their actual and predicted sizes, the crania of larger dormice are expected to  
260 have upper incisors that curve more posteriorly, an inferiorly angled rostrum, an increased maximum  
261 width of the zygomatic arch, and a relative narrowing of the auditory meatus (Figure 2). The predicted  
262 relative narrowing of the auditory meatus is seen in the fossil taxa, but other aspects of the actual  
263 shapes of the giants deviate from these predicted shapes: none show the predicted curvature in the  
264 incisors, and the proposed inferior angle of the rostrum is only evident in *Leithia melitensis*. The  
265 widening of the zygomatic arch is present within fossil giants, but is absent in the extant Formentera  
266 giants. Furthermore, the zygomatic widening in the fossil giants is located much more anteriorly than  
267 predicted.

268         Predicted mandibular morphology of giant dormice is also very different from their actual  
269 shapes. The predicted shapes show a very narrow and antero-posteriorly elongated structure, whereas  
270 the actual giants have robust mandibles, with the posterior part being greatly enlarged dorsoventrally.  
271 Although the PSvAS graph implies a best-fit for giant mandibular shapes similar to that of non-giant  
272 dormice, the large Procrustes distances between the fitted shape and the actual shape (Table S6)  
273 indicate this is not the result of isometric scaling. Instead, the giants exhibit some unique  
274 morphologies; e.g. distinct features in *L. melitensis* include a foreshortened and relatively straight  
275 lower incisor, an exceptionally large and unperforated angular process, a posteriorly located anterior  
276 margin of the masseteric ridge, and a vertically oriented coronoid process.

277         As the cranial and mandibular warps were created using the respective landmark  
278 configurations, features not included in the configuration, such as the shape of the auditory bullae,  
279 cannot be reliably assessed using the warped images. Figure S2 shows the positioning of the landmarks  
280 on the giants with regards to their predicted shapes. The width of the zygomatic plate, visible in lateral  
281 view, seems to increase with size in the fossil specimens. Furthermore, all giants appear to have a

282 sharply angled cranial vault. Lastly, we noticed a peculiar enlargement of the occipital condyle when  
283 observing the  $\mu$ CT scan of *H. morpheus*, not seen in other specimens.

284

## 285 **Discussion**

286 Extant giant Formentera dormice and fossil giant specimens of Sicily and Mallorca show substantial  
287 craniomandibular differences from their non-giant relatives (*Eliomys quercinus*; Figures 1 and S3). Only  
288 a small portion of these morphological differences can be explained by the allometric trajectories of  
289 non-giant populations. Insular giant dormice therefore diverge substantially from allometric  
290 expectations. Additionally, we recognized that different species of giant dormice show distinctive  
291 deviations from their predicted shapes.

292

### 293 *Predicting giant size and shape*

294 The cranial and mandibular morphologies of living and extinct island giants are different from those  
295 expected under an allometric model. Allometry-related aspects of the shapes of these giants are  
296 generally more similar to those of smaller dormice (although they also show substantial non-allometric  
297 shape differences), and this effect is more pronounced for the mandible than for the cranium (Figure  
298 1C,F). Although the craniomandibular shapes of giant dormice are more similar to smaller dormice  
299 than expected, this does not imply isometric scaling; the actual fit of the giants within the model is  
300 rather poor, and is worse for larger specimens (see Procrustes distances Table S6). Phylogenetically,  
301 the fossil specimens are more separated from the base model, potentially explaining the poor fit of  
302 these shapes within the model. The biologically implausible geometries that result from extrapolation  
303 of the allometric model to giant sizes provide an alternative explanation. For example, the predicted  
304 skull shape based on the cranial size of *L. melitensis* (log centroid size = 5.02) has an unrealistically  
305 flexed cranial vault and occipital region, including a highly constricted foramen magnum. A similarly  
306 unlikely morphology is evident for mandibular geometry, with the expected shape at the size of *L.*  
307 *melitensis* (log centroid size = 4.11) being implausible owing to the very thin mediolateral width of the

308 bone. Interestingly, the morphologies of smaller giants (Formentera population and *Hypnomys*) are  
309 not correctly predicted by the allometric base model either. These observations suggest that flattening  
310 or truncation of the allometric trajectory occurs at large size in order to maintain biological  
311 functionality.

312 Only part of the morphology of giant dormice can be explained by flattening of the allometric  
313 trajectory — large differences are also evident in comparison to their expected shapes based on  
314 (smaller) ‘best fit’ centroid sizes (Table S6; Figure 2). This indicates the presence of population-specific  
315 morphological features within island giants, potentially reflecting adaptive variation due to island-  
316 specific environmental conditions or ecological shifts. For example, the extant giant population of  
317 Formentera is noticeably more faunivorous compared to other populations [28]. This suggests either  
318 that insular body size increases have resulted in a dietary niche shift, or that a shift towards carnivory  
319 reflects insular selective pressures on Formentera and is the driver of evolutionary increases in body  
320 size. Although this is not the classic explanation of large body size in small mammals on islands [1], it  
321 indicates that morphological variation among dormouse populations could represent allometry and  
322 dietary (or other ecological) adaptations.

323

#### 324 *Morphological traits of giant dormice*

325 Cranial morphology of island giants clearly deviates from the allometric expectations, even when  
326 compared to their ‘predicted sizes’ (i.e. best-fit sizes to the line of allometry; Figure 2). The robust  
327 rostrum and narrowing of the infraorbital foramen within all fossil giants are not predicted by the  
328 allometric model at any cranial size. The model predicts the zygomatic arch in giants to become more  
329 enlarged posteriorly. In reality, the arch does get more robust, but its maximum width is located much  
330 more anteriorly. Larger dormice show a dorso-ventral flattening of the skull and changes to the  
331 posterior part of the mandible, such as an elongated coronoid process and enlarged condylar and  
332 angular processes. These are areas associated with masticatory muscle attachment [45], and their  
333 modification suggests relative increases in molar bite force [46,47] or gape [48,49]. Multiple studies

334 have already shown that small changes in cranial and mandibular size and shape can affect mechanical  
335 advantage and gape, both of which will impact the range of dietary items that can be processed. This  
336 effect has been shown in a number of mammalian groups [50-53] but is particularly well-studied in  
337 rodents [54-60]. The flattening of the skull is commonly seen in more rupicolous dormice [61],  
338 although it may also be product of enlarged body size owing to negatively allometric scaling of brain  
339 size [62] and craniofacial evolutionary allometry (CREA)[63]. This pattern, which is seen in many  
340 mammalian groups, predicts relatively smaller braincases and longer rostra in larger species [64,65].

341

#### 342 *Unique features of giant dormouse species*

343 Significant modifications to shape and size can result from evolutionary adaptation to novel ecologies,  
344 including new diets [22]. We therefore interpret the unique morphological features identified in the  
345 giant dormouse populations as reflecting specific ecological adaptations to insular settings. As well as  
346 diverging from the non-giant allometric trajectory, giant dormice also differ morphologically from one  
347 another. Such differences can be the result of various factors, including variation in ecosystem  
348 composition, ecological niche occupation, as well as duration of isolation on islands. The introduction  
349 of *Eliomys quercinus* to Formentera is thought to have occurred roughly 4000 years ago, whereas both  
350 *Hypnomys* and *Leithia* were isolated for millions of years. Even though the morphology of Formentera  
351 dormice does not resemble an intermediate shape between an average-sized *E. quercinus* and the  
352 fossil giants, the differences in duration of isolation are substantial. Many population-specific aspects  
353 of giant dormouse cranial, and especially mandibular, structure complement previous evidence of  
354 divergent dietary and other ecological traits in these taxa.

355

#### 356 *Formentera*

357 The Formentera dormice are the only extant giants and are morphologically different from the fossil  
358 giants. It is the only giant population retaining a large infraorbital foramen. Furthermore, the  
359 mandibular morphology of this population is characterised by a deep angular notch and relatively large



360 coronoid process, in contrast to the fossil giants. This enlarged coronoid results in a larger attachment  
361 area for the temporalis muscle, suggesting an increased incisor bite force, which would be  
362 advantageous for the extensive faunivorous behaviour observed within the Formentera population  
363 [28]. Previous research has suggested that faunivory, more than other diets, places unique pressures  
364 on rodents, driving greater morphological change [59,66]. However, this is not the case in the dormice  
365 studied here, with the Formentera population resembling non-giant dormice more than the other  
366 giants, based on the relatively short Procrustes distances of the best-fit in the PSvAS model (cranium  
367 0.07; mandible 0.06) (Table S6).

368

### 369 *Hypnomys*

370 The *Hypnomys* material in our dataset is much more robust than other dormice, with the exception  
371 of *Leithia melitensis*. The PSvAS model indicates that the morphology of this genus is substantially  
372 different from extant dormice (cranium 0.10; mandible 0.08). The *H. onicensis* specimen examined  
373 here is considered a subadult and is less robust than *H. morpheus*. The latter is characterised by  
374 exceptionally pronounced occipital condyles. The robust morphology of the zygomatic area and  
375 mandible in the two *Hypnomys* specimens indicates well developed masseteric musculature, which  
376 suggests a diet including tough foods for this genus. A more abrasive plant-based diet has also been  
377 suggested based on molar microwear [67].

378

### 379 *Leithia*

380 *Leithia melitensis* is the largest and most robust dormouse. *Hypnomys* and *Leithia* show similar  
381 morphological modifications, although these are often more pronounced within *Leithia* [32]. This also  
382 explains the relatively large Procrustes distances seen in the PSvAS model for this species (cranium  
383 0.13; mandible 0.12). In particular, the width of the rostrum and the zygomatic plate is exceptional.  
384 The mandible within this giant has very large angular and condylar processes. It is the only giant in  
385 which there appears to be no fenestration of the angular process. However, the functional significance

386 of this fenestra is unknown. The coronoid is deflected less posteriorly, resulting in a more upright  
387 position. The anterior margin of the masseteric ridge is positioned more posteriorly than in other  
388 dormice and the incisor is relatively short and curves less superiorly. The cranial and mandibular  
389 features seen in *L. melitensis*, in particular the exceptionally robust mandible, likely represent  
390 adaptations to a herbivorous diet [68], possibly explaining its extraordinary size. In addition,  
391 considerable variability in wear of the molar row is seen within the analysed fossil material of *L.*  
392 *melitensis* (Figure S4), indicating a relatively abrasive diet against which the molars were used  
393 extensively, also consistent with herbivory.

394

### 395 *Conclusion*

396 Multiple, independent dormice lineages achieved exceptional large size in insular habitats since the  
397 end of the Messinian Salinity Crisis (5.33 Ma [69]). Extrapolation of common allometry as an  
398 evolutionary line of least resistance on short timescales predicts that island giants could have highly  
399 similar craniomandibular morphologies. Moreover, a graded trend to gigantism as proposed by the  
400 island rule suggests that the importance of selective pressures within an ecosystem varies in a  
401 predictable manner [13,14]. However, we find that the morphologies of giant dormice are not an  
402 extrapolation along the allometric gradient of non-giant populations. This indicates that insular  
403 gigantism may lead to a deviation from the otherwise strong allometric conservatism suggested to  
404 exist in rodents [70]. Furthermore, the cranial and mandibular features of giant dormice contain a  
405 prominent population-specific component, illustrating divergence and inherently non-predictable  
406 adaptations to various different ecological niches, on different islands. These differences in the  
407 evolutionary pathways of island giants may reflect differences in ecosystem composition among  
408 islands and through geological time. Our findings have implications that extend beyond the study of  
409 giant dormice, suggesting that island adaptation may commonly involve ecological shifts that are  
410 unique and context-dependent, resulting in a high diversity of evolutionary responses to insular  
411 habitats in mammals.

412

### 413 **Acknowledgements**

414 We thank Cesar Espinoza Campuzano for discussions on predicted size models; Antonio Profico for his  
415 assistance with the R script; Pip Brewer, Roula Pappa and Roberto Portela-Miguez (NHMUK), Irina Ruf  
416 and Thomas Lehmann (SMF), Paolo Viscardi (NMI), Violaine Nicolas (MNHM), Carolina di Patti (G.G.  
417 Gemmellaro), Maria Rita Palombo (MUST), Letizia Del Favero and Mariagabriella Fornasiero (IGUP) and  
418 Loïc Costeur (NMBA) for collections access; Dan Sykes, Farah Ahmed, Brett Clark and Paul Ward  
419 (NHMUK MicroCT scanning & data retrieval). We especially thank Tom Davies at the scanning facility  
420 in Bristol, for the many hours spent scanning dormice.

421

### 422 **Funding Information**

423 JJH is funded by a PhD studentship from the Hull York Medical School. The European Federation of  
424 Experimental Morphology provided additional funding enabling the necessary visits to museum  
425 collections throughout Europe. Funding was also provided by the European Union's Horizon 2020  
426 research and innovation program 2014–2018 under grant agreement 677774 (European Research  
427 Council [ERC] Starting Grant: TEMPO) to RBB. The contribution of ET and JAA is a part of the Research  
428 Project CGL2016-79795-R funded by the Agencia Estatal de Investigación (Ministerio de Economía,  
429 Industria y Competitividad)/Fondo Europeo de Desarrollo Regional (FEDER).

430

### 431 **References**

- 432 1. Foster JB. 1964 Evolution of mammals on islands. *Nature* 202, 234–235.
- 433 2. Van Valen L. 1973 Pattern and the balance of nature. *Evol. Theory* 49, 31–49.
- 434 3. Freudenthal M. 1972 *Deinogalerix koenigswaldi* nov. gen., nov. spec., a giant insectivore from  
435 the Neogene of Italy. *Scripta Geol.* 14, 1-19.
- 436 4. Freudenthal M. 1976 Rodent stratigraphy of some Miocene fissure fillings in Gargano (prov.  
437 Foggia, Italy. *Scripta Geol.* 37, 1–23.

- 438 5. Daams R, Freudenthal M. 1985 *Stertomys laticrestatus*, a new glirid (dormice, Rodentia) from  
439 the insular fauna of Gargano (Prov. of Foggia, Italy). *Scripta Geol.* 77, 21–27.
- 440 6. Freudenthal M. 1985 Cricetidae (Rodentia) from the Neogene of Gargano (Prov. of Foggia,  
441 Italy). *Scripta Geol.* 77, 29–74.
- 442 7. Mazza P. 1987 *Prolagus apricenicus* and *Prolagus imperialis*: two new Ochotonids  
443 (Lagomorpha, Mammalia) of the Gargano (Southern Italy). *Boll. della Soc. Paleontol. Ital.* 26,  
444 233–243.
- 445 8. Angelone C. 2007 Messinian *Prolagus* (Ochotonidae, Lagomorpha) of Italy. *Geobios* 40, 407–  
446 421.
- 447 9. Quintana J, Köhler M, Moyà-Solà S. 2011 *Nuralagus rex*, gen. et sp. nov., an endemic insular  
448 giant rabbit from the Neogene of Minorca (Balearic Islands, Spain). *J. Vert. Paleontol.* 31, 231–  
449 240. doi: 10.1080/02724634.2011.550367.
- 450 10. Agustí J, Bover P, Alcover JA. 2012 A new genus of endemic cricetid (Mammalia, Rodentia)  
451 from the late Neogene of Mallorca (Balearic Islands, Spain). *J. Vert. Palaeontol.* 32, 722-726.
- 452 11. Case, TJ. 1978 A general explanation for insular body size trends in terrestrial  
453 vertebrates. *Ecology* 59, 1-18.
- 454 12. Heaney LR. 1978 Island area and body size of insular mammals: evidence from the tri-colored  
455 squirrel (*Callosciurus prevosti*) of Southeast Asia. *Evolution* 32, 29-44.
- 456 13. Lomolino MV. 1985 Body size of mammals on islands: the island rule reexamined. *Am. Nat.*  
457 125, 310-316.
- 458 14. Lomolino MV. 2005 Body size evolution in insular vertebrates: generality of the island rule. *J.*  
459 *Biogeogr.* 32, 1683-1699.
- 460 15. McNab BK. 2010 Geographic and temporal correlations of mammalian size reconsidered: a  
461 resource rule. *Oecologia* 164, 13-23.
- 462 16. van der Geer AA, Lyras GA, Lomolino MV, Palombo MR, Sax DF. 2013 Body size evolution of  
463 palaeo-insular mammals: temporal variations and interspecific interactions. *J. Biogeogr.* 40,

- 464 1440-1450.
- 465 17. van der Geer AA. 2014 Parallel patterns and trends in functional structures in extinct island  
466 mammals. *Integr. Zool.* 9, 167-182. doi: 10.1111/1749-4877.12066
- 467 18. Lomolino MV, van der Geer AA, Lyras GA, Palombo MR, Sax DF, Rozzi R. 2013 Of mice and  
468 mammoths: generality and antiquity of the island rule. *J. Biogeogr.* 40, 1427-1439.
- 469 19. Pélabon C, Firmat C, Bolstad GH, Voje KL, Houle D, Cassara J, Le Rouzic A, Hansen TF. 2014  
470 Evolution of morphological allometry. *Ann. NY Acad. Sci.* doi:10.1111/nyas.12470
- 471 20. Schluter D. 1996 Adaptive radiation along genetic lines of least resistance. *Evolution* 50, 1766–  
472 1774. doi:10.2307/2410734
- 473 21. Marroig G, Cheverud JM. 2010 Size as a line of least resistance II: direct selection on size or  
474 correlated response due to constraints? *Evolution: International Journal of Organic*  
475 *Evolution*, 64(5), 1470-1488. doi: 10.1111/j.1558-5646.2009.00920.x
- 476 22. Marroig G, Cheverud JM. 2001 A comparison of phenotypic variation and covariation patterns  
477 and the role of phylogeny. Ecology, and ontogeny during cranial evolution of New World  
478 monkeys. *Evolution* 55, 2576–2600. doi:10.1111/j.0014-3820.2001.tb00770.x
- 479 23. Huxley JS. 1932 Problems of relative growth. New York, NY: Dial Press.
- 480 24. Voje KJ, Hansen TF, Egset CK, Bolstad GH, Pélabon C. 2014 Allometric constraints and the  
481 evolution of allometry. *Evolution* 68, 866–885. doi:10.1111/evo.12312
- 482 25. Lister AM. 1989 Red deer dwarfing on Jersey in the last interglacial. *Nature* 342, 539– 542.
- 483 26. van der Geer AA, Lyras GA, de Vos J, Dermitzakis M. 2010 *Evolution of Island Mammals:*  
484 *Adaptation and Extinction of Placental Mammals on Islands*. Oxford, UK: Wiley-Blackwell  
485 Publishing.
- 486 27. Palombo MR. 2018 Insular mammalian fauna dynamics and paleogeography: a lesson from the  
487 western Mediterranean islands. *Integr. Zool.* 13, 2-20. doi: 10.1111/1749-4877.12275.
- 488 28. Kahmann H, Lau G. 1972 Der Gartenschläfer *Eliomys quercinus ophiusae* Thomas, 1925 von der  
489 Pityuseninsel Formentera (Lebensführung). *Veröffentlichungen der zoologischen*

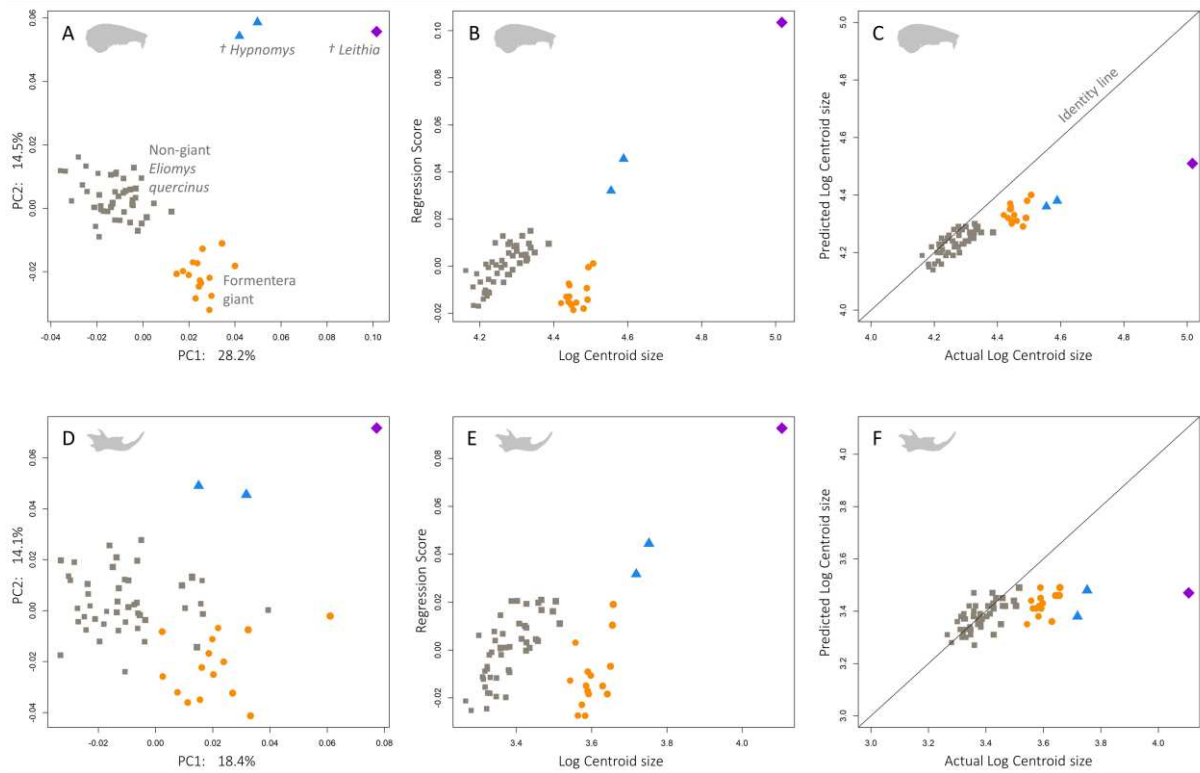
- 490           *Staatssammlung München* 16, 29-49.
- 491           29. Daams R, De Bruijn H. 1995 A classification of the Gliridae (Rodentia) on the basis of dental  
492           morphology. *Hystrix*, 6 (1-2), 3-50.
- 493           30. Freudenthal M, Martín-Suárez E. 2013 New ideas on the systematics of Gliridae (Rodentia,  
494           Mammalia). [Nuevas ideas sobre la sistemática de Gliridae (Rodentia, Mammalia)]. *Spanish J.*  
495           *Palaeont.* 28 (2), 239-252.
- 496           31. Bover P, Alcover JA, Michaux JJ, Hautier L, Hutterer R. 2010 Body shape and life style of the  
497           extinct Balearic dormouse *Hypnomys* (Rodentia, Gliridae): new evidence from the study of  
498           associated skeletons. *PLoS ONE* 5, e15817.
- 499           32. Hennekam JJ, Herridge VL, Costeur L, Di Patti C, Cox PG. 2020 Virtual cranial reconstruction of  
500           the endemic gigantic dormouse *Leithia melitensis* (Rodentia, Gliridae) from Poggio Schinaldo,  
501           Sicily. *Open Quat.* 6(1), 7. doi: <http://doi.org/10.5334/oq.79>
- 502           33. Orlandi-Oliveras G, Jordana X, Moncunill-Solé B, Köhler M. 2016 Bone histology of the giant  
503           fossil dormouse *Hypnomys onicensis* (Gliridae, Rodentia) from Balearic Islands. *C R Palevol* 15,  
504           238-244.
- 505           34. Mills DH. 1976 Osteological study of the Pleistocene dormouse *Hypnomus morpheus* Bate from  
506           Mallorca (Rodentia, Gliridae). *Publ. Paleontol. Inst. Univ. Uppsala* 4, 5-73.
- 507           35. Zelditch ML, Swiderski DL, Sheets HD. 2012 *Geometric morphometrics for biologists: a primer.*  
508           academic press.
- 509           36. Profico A, Veneziano A, Melchionna M, Raia P. 2018 Arothron: R functions for geometric  
510           morphometric analyses. R package version 1.0.0, [https://cran.r-](https://cran.r-project.org/web/packages/Arothron/index.html)  
511           [project.org/web/packages/Arothron/index.html](https://cran.r-project.org/web/packages/Arothron/index.html)
- 512           37. R Core Team, 2019. *R: A language and environment for statistical computing.* Vienna, Austria:  
513           R Foundation for Statistical Computing.
- 514           38. Rohlf FJ. 1990 Morphometrics. *Ann. Rev. Ecol. Syst.* 21, 299–316.
- 515           39. Mitteroecker P, Gunz P. 2009 Advances in geometric morphometrics. *J. Evol. Biol.* 36, 235–247.

- 516 doi: 10.1007/s11692-009-9055-x.
- 517 40. Schlager S. 2017 Morpho and Rvcg – shape analysis in R. In *Statistical Shape and Deformation*  
518 *Analysis* (eds G Zheng, S Li, GJ Székely), pp. 217–256. San Diego, CA: Academic Press.
- 519 41. Adams DC, Collyer ML, Kaliontzopoulou, A. 2018 Geomorph: Software for geometric  
520 morphometric analyses. R package version 3.0.6. [https://cran.r-](https://cran.r-project.org/package=geomorph)  
521 [project.org/package=geomorph](https://cran.r-project.org/package=geomorph).
- 522 42. Klingenberg CP. 2016 Size, shape, and form: concepts of allometry in geometric  
523 morphometrics. *Dev. Genes Evol.* 226, 113-137.
- 524 43. Drake AG, Klingenberg CP. 2007 The pace of morphological change: historical transformation  
525 of skull shape in St Bernard dogs. *Proc. R. Soc. B* 275, 71-76.
- 526 44. Mitteroecker P, Gunz P, Bernhard M, Schaefer K, Bookstein FL. 2004 Comparison of cranial  
527 ontogenetic trajectories among great apes and humans. *J. Human Evol.* 46, 679-698. doi:  
528 10.1016/j.jhevol.2004.03.006.
- 529 45. Cox PG, Jeffery N. 2015 The muscles of mastication in rodents and the function of the medial  
530 pterygoid. In *Evolution of the rodents: advances in phylogeny, functional morphology and*  
531 *development* (eds PG Cox, L Hautier), pp. 350-372. Cambridge, UK: Cambridge University Press.
- 532 46. Hiiemae KM. 1971 The structure and function of jaw muscles in the rat (*Rattus norvegicus* L.)  
533 III. The mechanics of the muscles. *Zool. J. Linn. Soc.* 50, 111-132.
- 534 47. Weijs WA, Dantuma R. 1975 Electromyography and mechanics of mastication in the albino rat.  
535 *J. Morphol.* 146, 1-33.
- 536 48. Vinyard CJ, Payseur BA. 2008 Of “mice” and mammals: utilizing classical inbred mice to study  
537 the genetic architecture of function and performance in mammals. *Integr. Comp. Biol.* 48, 324-  
538 337.
- 539 49. Cornette R, Herrel A, Cosson J-F, Poitevin F, Baylac M. 2012 Rapid morpho-functional changes  
540 among insular populations of the greater white-toothed shrew. *Biol. J. Linn. Soc.* 107, 322–331.
- 541 50. McIntosh AF, Cox PG. 2016 Functional implications of craniomandibular morphology in African

- 542 mole-rats (Rodentia: Bathyergidae). *Biol. J. Linn. Soc.* 117, 447-462.
- 543 51. Kiltie RA. 1982 Bite force as a basis for niche differentiation between rain forest peccaries  
544 (*Tayassu tajacu* and *T. pecari*). *Biotropica* 14, 188-195.
- 545 52. Herrel A, McBrayer LD, Larsen PM. 2007 Functional basis for sexual differences in bite force in  
546 the lizard *Anolis carolinensis*. *Biol. J. Linn. Soc.* 91, 111–119. doi: 10.1111/j.1095-  
547 8312.2007.00772.x
- 548 53. Herrel A, de Smet A, Aguirre LF, Aerts P. 2008 Morphological and mechanical determinants of  
549 bite force in bats: do muscles matter? *J. Exp. Biol.* 211, 86-91. doi: 10.1242/jeb.012211
- 550 54. Williams SH, Peiffer E, Ford S. 2009 Gape and bite force in the rodents *Onychomys leucogaster*  
551 and *Peromyscus maniculatus*: Does jaw-muscle anatomy predict performance? *J.*  
552 *Morphol.* 270, 1338-1347.
- 553 55. Cox PG, Rayfield EJ, Fagan MJ, Herrel A, Pataky TC, Jeffery N. 2012 Functional evolution of the  
554 feeding system in rodents. *PLoS ONE* 7, e36299. doi: 10.1371/journal.pone.0036299.
- 555 56. Renaud S, Gomes Rodrigues HG, Ledevin R, Pisanu B, Chapuis J-L, Hardouin EA. 2015 Fast  
556 evolutionary response of house mice to anthropogenic disturbance on a Sub-Antarctic island.  
557 *Biol. J. Linn. Soc.* 114, 513–526.
- 558 57. McIntosh AF, Cox PG. 2016 Functional implications of craniomandibular morphology in African  
559 mole-rats (Rodentia: Bathyergidae). *Biol. J. Linn. Soc.* 117, 447–462.
- 560 58. Cox, PG, Morris PJR, Hennekam JJ, Kitchener AC. 2020 Morphological and functional variation  
561 between isolated populations of British red squirrels. *J. Zool.* doi: 10.1111/jzo.12829
- 562 59. Fabre P-H, Herrel A, Fitriana Y, Meslin L, Hautier L. (2017). Masticatory muscle architecture in  
563 a water-rat from Australasia (Murinae, Hydromys) and its implication for the evolution of  
564 carnivory in rodents. *J. Anat.* 231(3), 380-397.
- 565 60. Ginot S, Herrel A, Claude J, Hautier L. 2018 Skull size and biomechanics are good estimators of  
566 in vivo bite force in murid rodents. *Anat. Rec.* 301, 256-266.
- 567 61. Holden-Musser ME, Juškaitis R, Musser GM. 2016 Gliridae. In *Handbook of the Mammals of*



- 568            *the World. Volume 6: Lagomorphs and Rodents I* (eds DE Wilson, TE Lacher, RA Mittermeier),  
569            pp. 838-889. Barcelona, Spain: Lynx Edicions.
- 570            62. Penrose F, Kemp GJ, Jeffery N. 2016 Scaling and accommodation of jaw adductor muscles in  
571            Canidae. *Anat. Rec.* 299, 951-966.
- 572            63. Cardini A, Polly D, Dawson R, Milne N. 2015 Why the long face? Kangaroos and wallabies follow  
573            the same 'rule' of cranial evolutionary allometry (CREA) as placentals. *J. Evol. Biol.* 42(2), 169–  
574            176. doi: 10.1007/s11692-015-9308-9
- 575            64. Radinsky LB. 1985 Approaches in evolutionary morphology: A search for patterns. *Annu Rev*  
576            *Ecol Evol Syst.* 16(1), 1–14. <https://doi.org/10.1146/annurev.es.16.110185.000245>
- 577            65. Cardini, A. 2019 Craniofacial allometry is a rule in evolutionary radiations of placentals. *J. Evol.*  
578            *Biol.* 46(3), 239-248.
- 579            66. Maestri R, Patterson BD, Fornel R, Monteiro LR, De Freitas TRO. 2016 Diet, bite force and skull  
580            morphology in the generalist rodent morphotype. *J. Evol. Biol.*, 29(11), 2191-2204.
- 581            67. Hautier L, Bover P, Alcover JA, Michaux J. 2009 Mandible morphometrics, dental microwear  
582            pattern, and paleobiology of the extinct Balearic dormouse *Hypnomys morpheus*. *Acta*  
583            *Palaeontol. Pol.* 54, 181-194.
- 584            68. Michaux J, Chevret P, Renaud S. 2007 Morphological diversity of Old World rats and mice  
585            (Rodentia, Muridae) mandible in relation with phylogeny and adaptation. *J. Zool. Syst. Evol.*  
586            *Res.* 45, 263-279.
- 587            69. Krijgsman W, Hilgen FJ, Raffi I, Sierro FJ, Wilson DS. 1999 Chronology, causes and progression  
588            of the Messinian salinity crisis. *Nature*, 400(6745), 652-655.
- 589            70. Wilson LA. 2013 Allometric disparity in rodent evolution. *Ecol. Evol.* 3, 971-984.
- 590  
591  
592  
593



594

595

596 Figure 1: Cranial (top) and mandibular (bottom) shape differentiation in extant *Eliomys quercinus*  
 597 specimens and fossil giants on the first two principal components (A,D); the common allometric  
 598 component versus log centroid size with grouping (B,E); and the predicted size versus actual size  
 599 analyses based on a non-giant base model including the predicted sizes for the giant Formentera  
 600 population and fossil giants (C,F).

601

602

603

604

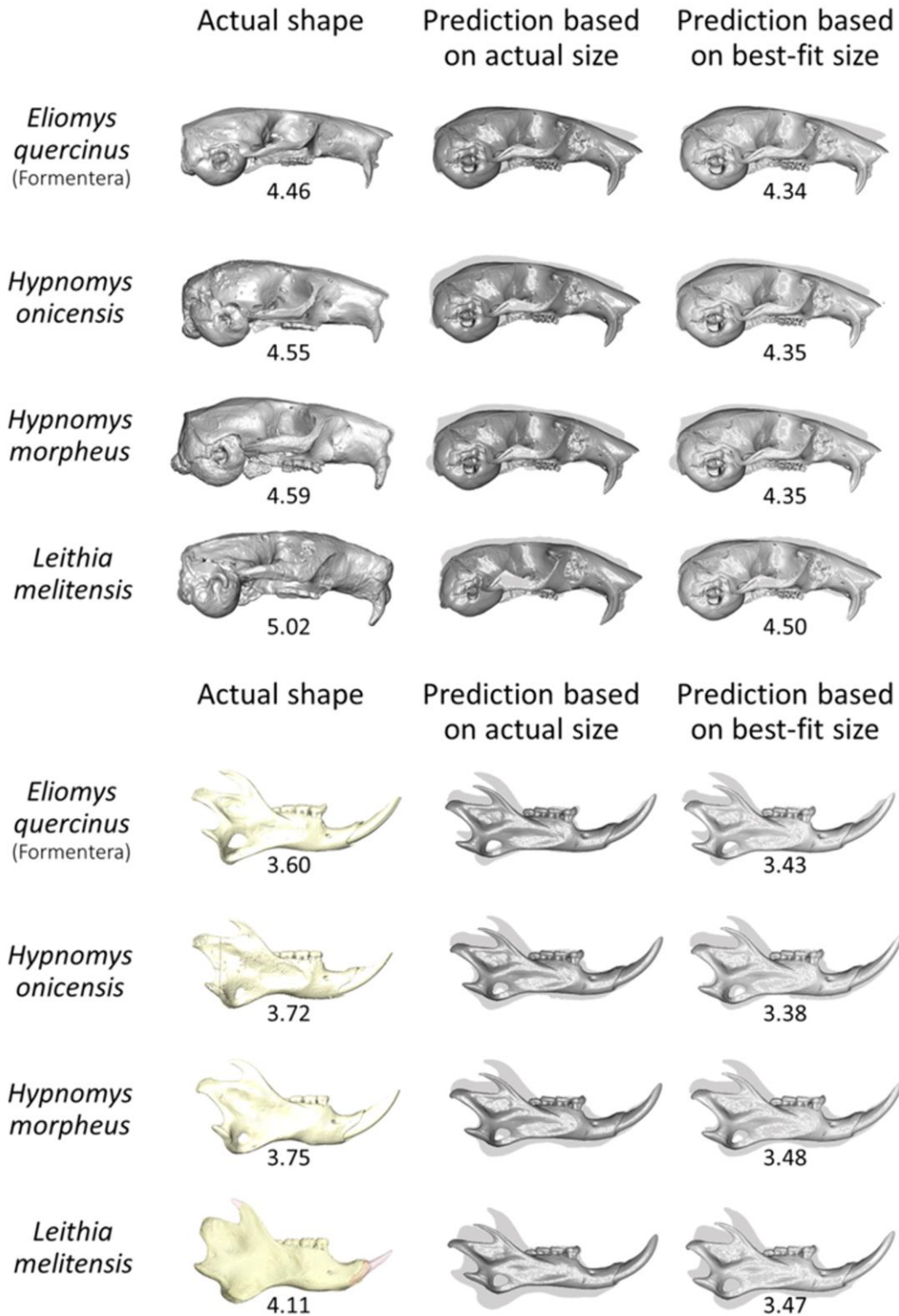
605

606

607

608

609



610

611 Figure 2: Predicted shapes of the fossil giants derived from the PSvAS model, using the shape

612 predicted by the actual centroid size of the specimen and the shape presumed to be the best fit with

613 the actual shape of the specimen.